

Shot noise of quantum ring excitons in a planar microcavity

Y. N. Chen, D. S. Chuu, and S. J. Cheng

Department of Electrophysics, National Chiao-Tung University, Hsinchu 300, Taiwan

(Received 25 July 2005; revised manuscript received 5 September 2005; published 1 December 2005)

Shot noise of quantum ring (QR) excitons in a p-i-n junction surrounded by a microcavity is investigated theoretically. Some radiative decay properties of a QR exciton in a microcavity can be obtained from the observation of the current noise, which also gives extra information about one of the tunnel barriers. A different noise feature between the quantum dot (QD) and QR is pointed out, and may be observed in a suitably designed experiment.

 DOI: [10.1103/PhysRevB.72.233301](https://doi.org/10.1103/PhysRevB.72.233301)

PACS number(s): 71.35.-y, 73.63.-b, 73.50.Td, 42.50.Pq

Since Purcell proposed the idea of controlling the spontaneous emission rate by using a cavity,¹ the enhanced and inhibited SE rate for the atomic system was intensively investigated in the 1980s² by using atoms passed through a cavity. In semiconductor systems, the electron-hole pair is naturally a candidate to examine the spontaneous emission. Modifications of the SE rates of the quantum dot (QD),³ quantum wire,⁴ or quantum well⁵ excitons inside the microcavities have been observed experimentally.

Interest in measurements of shot noise spectrum has risen owing to the possibility of extracting valuable information not available in conventional dc transport experiments.⁶ With the advances of fabrication technologies, it is now possible to embed the QDs inside a p-i-n structure⁷ such that the electron and hole can be injected separately from opposite sides. This allows one to examine the exciton dynamics in a QD via electrical currents.⁸ On the other hand, it is now possible to fabricate the ring-shaped dots of InAs in GaAs with a circumference of several hundred nanometers.⁹ Optical detection of the Aharonov-Bohm effect on an exciton in a single quantum ring (QR) was also reported.¹⁰

Based on the rapid progress of nanotechnologies, it is not hard to imagine that the QR can be incorporated in a p-i-n junction surrounded by the microcavity. Examinations of the dynamics of the QR excitons by the electrical currents can be realized. We thus present in this work the nonequilibrium calculations of such a device. Current noise of QR excitons in a planar microcavity is obtained via the MacDonald formula¹¹ and is found to reveal some characteristics of the restricted environment, i.e., the density of states of the confined photons.

The model. Consider now a QR embedded in a p-i-n junction as shown in Fig. 1. Both the hole and electron reservoirs are assumed to be in thermal equilibrium. For the physical phenomena we are interested in, the Fermi level of the $p(n)$ -side hole (electron) is slightly lower (higher) than the hole (electron) subband in the dot. After a hole is injected into the hole subband in the QR, the n -side electron can tunnel into the exciton level because of the Coulomb interaction between the electron and hole. Thus, we may introduce the three ring states; $|0\rangle=|0,h\rangle$, $|\uparrow\rangle=|e,h\rangle$, and $|\downarrow\rangle=|0,0\rangle$, where $|0,h\rangle$ means there is one hole in the QR, $|e,h\rangle$ is the exciton state, and $|0,0\rangle$ represents the ground state with no hole and electron in the QR. One might argue

that one cannot neglect the state $|e,0\rangle$ for real device since the tunable variable is the applied voltage. This can be resolved by fabricating a thicker barrier on the electron side so that there is little chance for an electron to tunnel in advance. Moreover, the charged exciton and biexcitons states are also neglected in our calculations. This means a low injection limit is required in the experiment.⁷

Derivation of a master equation. We can now define the ring-operators $\hat{n}_\uparrow \equiv |\uparrow\rangle\langle\uparrow|$, $\hat{n}_\downarrow \equiv |\downarrow\rangle\langle\downarrow|$, $\hat{p} \equiv |\uparrow\rangle\langle\downarrow|$, $\hat{s}_\uparrow \equiv |0\rangle\langle\uparrow|$, $\hat{s}_\downarrow \equiv |0\rangle\langle\downarrow|$. The total Hamiltonian H of the system consists of three parts; H_0 [ring, photon bath H_p , and the electron (hole) reservoirs H_{res}], H_T (ring-photon coupling), and the ring-reservoir coupling H_V

$$H = H_0 + H_T + H_V,$$

$$H_0 = \varepsilon_\uparrow \hat{n}_\uparrow + \varepsilon_\downarrow \hat{n}_\downarrow + H_p + H_{res},$$

$$H_T = \sum_k (D_k \hat{b}_k^\dagger \hat{p} + D_k^* \hat{b}_k \hat{p}^\dagger) = \hat{p} X + \hat{p}^\dagger X^\dagger,$$

$$H_p = \sum_k \omega_k \hat{b}_k^\dagger \hat{b}_k,$$

$$H_V = \sum_{\mathbf{q}} (V_{\mathbf{q}} \hat{c}_{\mathbf{q}}^\dagger \hat{s}_\uparrow + W_{\mathbf{q}} \hat{d}_{\mathbf{q}}^\dagger \hat{s}_\downarrow + \text{c.c.}),$$

$$H_{res} = \sum_{\mathbf{q}} \varepsilon_{\mathbf{q}} \hat{c}_{\mathbf{q}}^\dagger \hat{c}_{\mathbf{q}} + \sum_{\mathbf{q}} \varepsilon_{\mathbf{q}} \hat{d}_{\mathbf{q}}^\dagger \hat{d}_{\mathbf{q}}. \quad (1)$$

In the above equation, b_k is the photon operator, D_k is the dipole coupling strength, $X = \sum_k D_k \hat{b}_k^\dagger$, and $c_{\mathbf{q}}$ and $d_{\mathbf{q}}$ denote the electron operators in the left and right reservoirs, respectively. The couplings to the electron and hole reservoirs are given by the standard tunnel Hamiltonian H_V , where $V_{\mathbf{q}}$ and $W_{\mathbf{q}}$ couple the channels \mathbf{q} of the electron and the hole reservoirs. If the couplings to the electron and the hole reservoirs are weak, then it is reasonable to assume that the standard Born-Markov approximation with respect to these couplings is valid. In this case, one can derive a master equation from the exact time evolution of the system. The equations of motion can be expressed as (cf. Ref. 12)

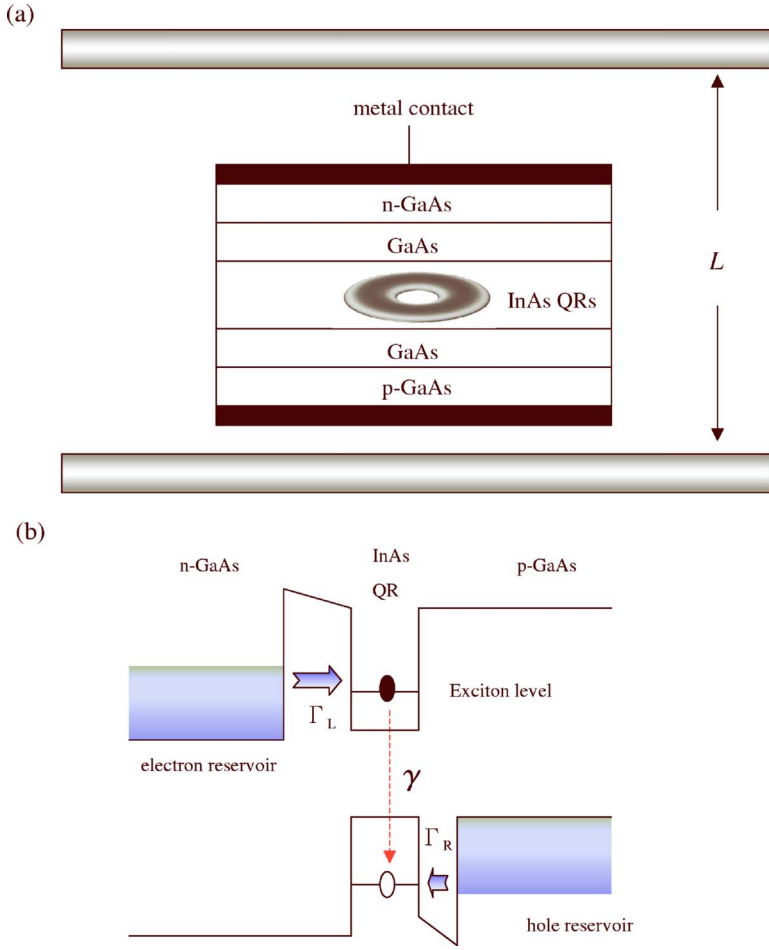


FIG. 1. (Color online) (a) Schematic description of a QR inside a p-i-n junction surrounded by a planar microcavity with length L . (b) Energy-band diagram of a QR in the p-i-n junction.

$$\begin{aligned}
 \frac{\partial}{\partial t} \langle \hat{n}_{\uparrow} \rangle_t &= - \int dt' [C(t-t') + C^*(t-t')] \langle \hat{n}_{\uparrow} \rangle_{t'} \\
 &\quad + \Gamma_L [1 - \langle \hat{n}_{\uparrow} \rangle_t - \langle \hat{n}_{\downarrow} \rangle_t], \\
 \frac{\partial}{\partial t} \langle \hat{n}_{\downarrow} \rangle_t &= \int dt' [C(t-t') + C^*(t-t')] \langle \hat{n}_{\uparrow} \rangle_{t'} - \Gamma_R \langle \hat{n}_{\downarrow} \rangle_t, \\
 \frac{\partial}{\partial t} \langle \hat{p} \rangle_t &= - \frac{1}{2} \int dt' [C(t-t') + C^*(t-t')] \langle \hat{p} \rangle_{t'} - \frac{\Gamma_R}{2} \langle \hat{p} \rangle_t,
 \end{aligned} \tag{2}$$

where $\Gamma_L = 2\pi \sum_{\mathbf{q}} V_{\mathbf{q}}^2 \delta(\varepsilon_{\uparrow} - \varepsilon_{\mathbf{q}}^{\uparrow})$, $\Gamma_R = 2\pi \sum_{\mathbf{q}} W_{\mathbf{q}}^2 \delta(\varepsilon_{\downarrow} - \varepsilon_{\mathbf{q}}^{\downarrow})$, and $\varepsilon = \varepsilon_{\uparrow} - \varepsilon_{\downarrow}$ is the energy gap of the QR exciton. Here, $C(t-t') \equiv \langle X_t X_{t'}^{\dagger} \rangle_0$ is the photon correlation function, and depends on the time interval only. We can now define the Laplace transformation for real z ,

$$\begin{aligned}
 C_{\varepsilon}(z) &\equiv \int_0^{\infty} dt e^{-zt} e^{i\varepsilon t} C(t), \\
 n_{\uparrow}(z) &\equiv \int_0^{\infty} dt e^{-zt} \langle \hat{n}_{\uparrow} \rangle_t \text{ etc.}, \quad z > 0,
 \end{aligned} \tag{3}$$

and transform the whole equations of motion into z space,

$$\begin{aligned}
 n_{\uparrow}(z) &= - [C_{\varepsilon}(z) + C_{\varepsilon}^*(z)] n_{\uparrow}(z) / z + \frac{\Gamma_L}{z} [1/z - n_{\uparrow}(z) - n_{\downarrow}(z)], \\
 n_{\downarrow}(z) &= [C_{\varepsilon}(z) + C_{\varepsilon}^*(z)] n_{\downarrow}(z) / z - \frac{\Gamma_R}{z} n_{\downarrow}(z), \\
 p(z) &= - \frac{1}{2} [C_{\varepsilon}(z) + C_{\varepsilon}^*(z)] p(z) / z - \frac{\Gamma_R}{2z} p(z).
 \end{aligned} \tag{4}$$

These equations can then be solved algebraically, and the tunnel current from the hole- or electron-side barrier

$$\hat{I}_R = -e \Gamma_R \langle \hat{n}_{\downarrow} \rangle_t, \quad \hat{I}_L = -e \Gamma_L [1 - \langle \hat{n}_{\uparrow} \rangle_t - \langle \hat{n}_{\downarrow} \rangle_t] \tag{5}$$

can then be obtained by performing the inverse Laplace transformation on Eqs. (4).

Shot noise spectrum. In a quantum conductor in nonequilibrium, electronic current noise originates from the dynamical fluctuations of the current being away from its average. To study correlations between carriers, we relate the exciton dynamics with the hole reservoir operators by introducing the degree of freedom n as the number of holes that have tunneled through the hole-side barrier¹³ and write

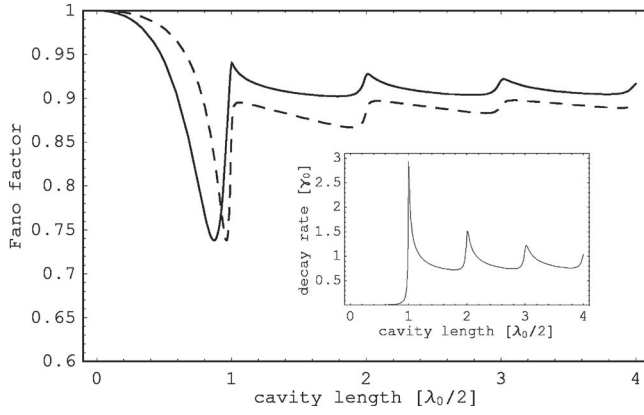


FIG. 2. Fano factor as a function of cavity length L . The vertical and horizontal units are $[S_{I_R}(0)]/(2eI)$ and $\lambda_0/2$, respectively. The inset shows the radiative decay rate of a QR exciton in a planar microcavity.

$$\begin{aligned} \dot{n}_0^{(n)}(t) &= -\Gamma_L n_0^{(n)}(t) + \Gamma_R n_{\downarrow}^{(n-1)}(t), \\ \dot{n}_{\uparrow}^{(n)}(t) + \dot{n}_{\downarrow}^{(n)}(t) &= (\Gamma_L - \Gamma_R) n_0^{(n)}(t). \end{aligned} \quad (6)$$

Equation (6) allows us to calculate the particle current and the noise spectrum from $P_n(t) = n_0^{(n)}(t) + n_{\uparrow}^{(n)}(t) + n_{\downarrow}^{(n)}(t)$ which gives the total probability of finding n electrons in the collector by time t . In particular, the noise spectrum S_{I_R} can be calculated via the MacDonald formula.¹⁴ In the zero-frequency limit, the Fano factor can be written as

$$F \equiv \frac{S_{I_R}(\omega=0)}{2e\langle I \rangle} = 1 - \frac{A(z)\Gamma_L\Gamma_R[A(z) + 2(\Gamma_L + \Gamma_R)]}{\{A(z)\Gamma_R + \Gamma_L[A(z) + 2\Gamma_R]\}^2} \Big|_{z=0}, \quad (7)$$

where $A(z) \equiv C_e(z) + C_e^*(z)$.

Results and Discussions. From Eq. (7), one knows that the noise spectrum of the QR excitons depends strongly on $C_e(z)$, which reduces to the radiative decay rate γ in the Markovian limit. The exciton decay rate γ in a microcavity can be obtained easily from the perturbation theory and is given by

$$\begin{aligned} \gamma &= \frac{e^2 \hbar \rho}{m^2 c d} \int |H_0^{(1)}| \\ &\times \langle (q' \rho)^2 q' \left(\sum_{k'_z} \frac{\delta(\varepsilon - c\sqrt{q'^2 + k_z'^2})}{\sqrt{k_z'^2 + q'^2}} |\epsilon_{q'k'_z\lambda} \cdot \chi|^2 \right) dq', \end{aligned} \quad (8)$$

where ρ is the ring radius, d is the lattice spacing, $H_0^{(1)}$ is the Hankel function, $\epsilon_{q'k'_z\lambda}$ is the polarization of the photon, and χ is the dipole moment of the QR exciton.¹⁵ The summation of the integer modes in the k'_z direction is determined from the boundary conditions of the planar microcavity.

The radiative decay rate γ of a QR exciton inside a planar microcavity is numerically displayed in the inset of Fig. 2. The tunneling rates, Γ_L and Γ_R , are assumed to be equal to $0.1\gamma_0$ and γ_0 , where γ_0 ($\sim 1/1$ ns) is the decay rate of a QR

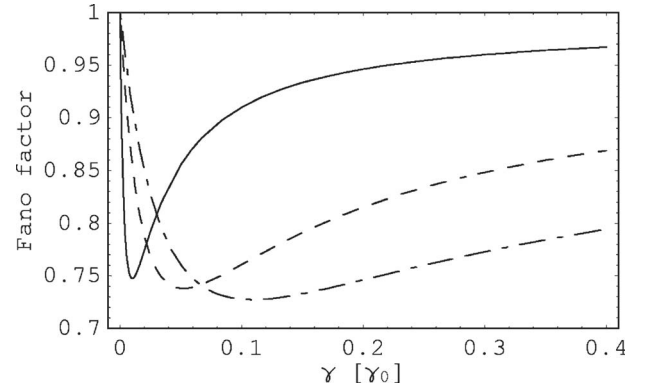


FIG. 3. Fano factor as a function of the decay rate for different electron-side tunneling rate $\Gamma_L = 0.01\gamma_0$ (solid line), $0.05\gamma_0$ (dashed line), and $0.1\gamma_0$ (dashed-dotted line). The hole-side tunneling rate is fixed ($\Gamma_R = \gamma_0$).

exciton in free space. Also, the planar microcavity is assumed to have a Lorentzian broadening at each resonant mode (with broadening width equal to 1% of each resonant mode).¹⁶ As the cavity length is shorter than one half the wavelength of the emitted photon ($L < \lambda_0/2$), the decay rate is inhibited because of the cut-off frequency of the cavity. When the cavity length exceeds some multiple wavelength, it opens up another decay channel for the quantum ring exciton and turns out that there is an abrupt enhancement on the decay rate. Such a singular behavior also happens in the decay of one dimensional quantum wire polaritons inside a microcavity.¹⁶ This is because the ring geometry preserves the angular momentum of the exciton, rendering the formation of exciton-polariton in the direction of circumference. This kind of behavior can also be found in the calculations of a Fano factor as demonstrated by the solid line in Fig. 2. Comparing to the zero-frequency noise of the QD excitons (dashed line), the Fano factor of the QR excitons shows the “cusp” feature at each resonant mode.

Another interesting point is that below the lowest resonant mode ($L = \lambda_0/2$), both the solid and dashed curves have a dip in the Fano factor. It is not seen from the radiative decay rate. To answer this, we have plotted Eq. (7) in Fig. 3 as a function of the decay rate γ . Keeping Γ_R unchanged, the solid, dashed, and dashed-dotted lines correspond to the electron-side tunneling rate $\Gamma_L = 0.01\gamma_0$, $0.5\gamma_0$, and $0.1\gamma_0$, respectively. As can be seen, the Fano factor has a minimum point at $\gamma = \Gamma_L\Gamma_R(\Gamma_L + \Gamma_R)/(\Gamma_L^2 + \Gamma_R^2)$. Comparing this with the inset of Fig. 2, one immediately knows that when the cavity length is increased to $\lambda_0/2$, the abruptly increased decay rate will cross the minimum point and result in a dip in Fig. 2. Furthermore, in the limit of $\Gamma_R \gg \Gamma_L$, the minimum point can be approximated as $\gamma \approx \Gamma_L$. This means by observing the dip in the Fano factor of Fig. 2, the magnitude of the electron-side tunneling rate Γ_L can be obtained.

To further understand the difference between the QD and QR excitons, Fig. 4 illustrates the shot noise as a function of energy gap ε . In plotting the figure, a perfect planar microcavity is assumed for convenience. As can be seen, the shot noise of the QD excitons shows the plateau feature (solid line) with the increasing of ε , while it is a zigzag behavior

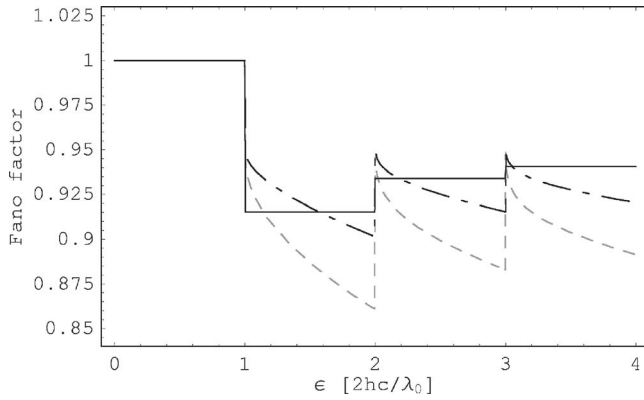


FIG. 4. Fano factor of QD (solid line) and QR (gray dashed line) excitons as a function of energy gap ε . The vertical and horizontal units are $[S_{I_R}(0)]/(2eI)$ and $2hc/\lambda_0$, respectively. The dashed-dotted line represents that if the free-space decay rate of the QR exciton is enhanced by a factor of $2(\gamma_0 \rightarrow 2\gamma_0)$, the shot noise is also enhanced.

(gray-dashed and dashed-dotted lines) for the QR excitons. This is because the decay rate of the QD exciton in a microcavity is given by¹⁶

$$\gamma_{dot} \propto \sum_{n_c} \frac{e^2 \hbar}{m^2 c^2 L} \theta[(\varepsilon/\hbar c)^2 - (\pi n_c / L)^2] |\epsilon_{q'k'_z} \cdot \chi|^2, \quad (9)$$

where θ is the step function, and the summation is over the positive integers. Therefore, when the energy gap ε is tuned above some resonant mode of the cavity, the decay rate is a constant before the next decay channel is opened. On the other hand, however, one knows that the decay rate for the QR exciton is not a constant between two resonant modes. This explains why the decay property for QR exciton is different from that for the QD exciton under the same photonic environment, and the difference may be distinguished by the shot noise measurements. From the experimental point of

view, different dependences on ε are easier to be realized since it is almost impossible to vary the cavity length once the sample is prepared. A possible way to observe the mentioned effects is to vary ε around the discontinuous points and measure the corresponding current noise.

A few remarks about the ring radius should be mentioned here. One should note that we do not give the specific value of the ring radius in our model. Instead, a phenomenological value about the free space decay rate γ_0 is used. The magnitudes of the tunnel rates are set relative to it. In general, the changing of radius will certainly affect the shot noise. For example, because of the exciton-polariton (super radiant) effect in the direction of circumference, an increasing of ring radius will enhance the decay rate. In addition, the dipole moment of the QR exciton χ is also altered because of the varying of the wave function. All these can contribute to the variations of the decay rate and shot noise. In our previous study,¹⁵ we have shown that the decay rate is a monotonic increasing function on radius ρ if the exciton is coherent in the quantum ring, i.e., free of scattering from impurities or imperfect boundaries. The dashed-dotted line in Fig. 4 shows the result for *doubled* free-space decay rate, i.e., $\gamma_0 \rightarrow 2\gamma_0$. Although the noise is increased, the zigzag feature remains unchanged.

In conclusion, we have derived in this work the nonequilibrium current noise of QR excitons incorporated in a p-i-n junction surrounded by a planar microcavity. Some radiative decay properties of the one-dimensional QR exciton can be obtained from the observation of shot noise spectrum, which also shows extra information about the electron-side tunneling rate. Different noise features between the QD and QR are pointed out, and deserve to be tested with present technologies.

This work is supported partially by the National Science Council, Taiwan under Grant Nos. NSC 94-2112-M-009-019 and NSC 94-2120-M-009-002.

¹E. M. Purcell, Phys. Rev. **69**, 681 (1946).

²P. Goy *et al.*, Phys. Rev. Lett. **50**, 1903 (1983); G. Gabrielse and H. Dehmelt, *ibid.* **55**, 67 (1985); R. G. Hulet *et al.*, *ibid.* **55**, 2137 (1985); D. J. Heinzen *et al.*, *ibid.* **58**, 1320 (1987).

³J. M. Gerard *et al.*, Phys. Rev. Lett. **81**, 1110 (1998); M. Bayer *et al.*, *ibid.* **86**, 3168 (2001); G. S. Solomon *et al.*, *ibid.* **86**, 3903 (2001).

⁴C. Constantin *et al.*, Phys. Rev. B **66**, 165306 (2002).

⁵G. Bjork *et al.*, Phys. Rev. A **44**, 669 (1991); K. Tanaka *et al.*, Phys. Rev. Lett. **74**, 3380 (1995).

⁶C. W. J. Beenakker, Rev. Mod. Phys. **69**, 731 (1997); Y. M. Blanter and M. Buttiker, Phys. Rep. **336**, 1 (2000).

⁷Z. Yuan *et al.*, Science **295**, 102 (2002); G. Kießlich *et al.*, Phys. Rev. B **68**, 125331 (2003).

⁸Y. N. Chen *et al.*, Phys. Rev. B **69**, 245323 (2004).

⁹R. J. Warburton *et al.*, Nature (London) **405**, 926 (2000).

¹⁰M. Bayer *et al.*, Phys. Rev. Lett. **90**, 186801 (2003).

¹¹D. K. C. MacDonald, Rep. Prog. Phys. **12**, 56 (1948).

¹²T. Brandes and B. Kramer, Phys. Rev. Lett. **83**, 3021 (1999); Y. N. Chen *et al.*, *ibid.* **90**, 166802 (2003).

¹³Actually, the total current noise should be expressed in terms of the spectra of particle currents and the charge noise spectrum: $S_I(\omega) = aS_{I_L}(\omega) + bS_{I_R}(\omega) - ab\omega^2 S_Q(\omega)$, where a and b are capacitance coefficient ($a+b=1$) of the junctions. Since we have assumed a highly asymmetric set up ($a \ll b$), it is plausible to consider the hole-side spectra $S_{I_R}(\omega)$ only.

¹⁴R. Aguado and T. Brandes, Phys. Rev. Lett. **92**, 206601 (2004).

¹⁵Y. N. Chen and D. S. Chuu, Solid State Commun. **130**, 491 (2004).

¹⁶Y. N. Chen *et al.*, Phys. Rev. B **64**, 125307 (2001).